A MPPT ALGORITHM FOR PARTIAL SHADING CONDITIONS EMPLOYING CURVE FITTING

Efstratios BATZELIS[(1)] Georgios KAMPITSIS[(2)] Stavros PAPATHANASSIOU[(3)]

National Technical University of Athens, Electric Power Division, 9 Iroon Politechneiou st., 15780, Athens, Greece
[(1)]batzelis@mail.ntua.gr,[(2)]gkampit@central.ntua.gr,[(3)]st@power.ece.ntua.gr

ABSTRACT: Standard maximum power point tracking (MPPT) algorithms often fail to locate the global maximum of a photovoltaic (PV) system under partial shading conditions, while other more sophisticated approaches usually involve extra perturbation of the operating point, which entails undesired output power fluctuation. In this paper, a new MPPT method is introduced, which continuously detects the shading parameters and estimates all power peaks (MPPs) on the *P-V* curve, guaranteeing continuous operation at the global maximum. The algorithm applies least squares (LSQ) curve fitting (CF) to measurements at the current MPP, utilizing the inherent ripple, without the need for additional perturbation on the operating point. The calculations performed are entirely mathematical and no extra measurement equipment is required, such as irradiance or temperature sensors. The method is designed for PV strings illuminated at two irradiance levels.
Keywords: Curve fitting, global maximum, least squares (LSQ), Levenberg-Marquardt, maximum power point (MPP), maximum power point tracking (MPPT), partial shading, photovoltaic (PV), power peaks.

1 INTRODUCTION

Several local maximum power points (MPPs) arise on the *P-V* curve of a photovoltaic (PV) string, when operating under partial shading conditions. Standard MPP tracking (MPPT) methods, like Perturb & Observe (P&O) or Incremental Conductance (INC), often fail to locate the global maximum and lock to a suboptimal MPP, leading to significant power losses.

There are some more sophisticated approaches in literature especially designed for partial shading, which are based on empirical formulae or evolutionary optimization algorithms [1]–[5]. Yet, all these methods involve periodic perturbation of the operating point, leading to undesirable fluctuation in the output power and extra power losses. In order to balance the pros and cons, the execution frequency of these algorithms is adjusted accordingly in these papers, still compromising between losses due to partial shading and the aforementioned implications.

A relevant global MPPT (GMPPT) strategy that avoids this kind of perturbation is presented in [6], which monitors the power peaks on the *P-V* curve and switches from one local MPP to another whenever needed in order to ensure operation at the global MPP. It utilizes measurements of the terminal voltage and current of the PV string at the actual operating MPP in order to mathematically estimate the shading conditions and evaluate the voltage and current of all MPPs. However, this method is designed for nominal temperature and assumes that the intensity of a particular shading event remains constant, which limits the universal applicability.

These restrictions arise from the use of only the operating voltage and current as input data, from which only two shading parameters can be determined by the equations in [6]. In this paper, this concept is enhanced employing least squares (LSQ) curve fitting (CF) on a larger set of voltage and current samples. The inherent switching ripple and perturbation introduced by a constantly running P&O algorithm are utilized, and the shading parameters and properties of all MPPs are estimated. This is a purely mathematical procedure that introduces no additional variation of the operating point, thus permitting frequent execution in order to keep track of very fast shading variations (duration of a few seconds). The proposed technique does not require an irradiance sensor or other additional components and is designed for PV strings illuminated at two irradiance levels. Its effectiveness is validated and compared to a typical P&O approach via simulations in MATLAB/Simulink.

2 PV STRING MODELING UNDER PARTIAL SHADING CONDITIONS

A PV string consists of several PV modules connected in series, while a PV module comprises series connected PV cells. A group of series connected cells within a module, with a bypass diode connected in parallel at its terminals, is denoted a *cell string*. Under partial shading conditions, assuming two irradiance levels (i.e. one level of shade), the shaded cell strings are illuminated at irradiance G_{sh}, while the unshaded ones at irradiance G_{un} ($G_{un}>G_{sh}$). The shaded and unshaded parts of the string (denoted as *cell string groups*) comprise N_{sh} and N_{un} cell strings respectively ($N_{tot}=N_{sh}+N_{un}$).

As explained in [7], [8], in such conditions up to two MPPs may appear on the *P-V* curve of the string, denoted MPP1 and MPP2. An indicative case is illustrated in Figure 1(a)-(b). When operating at MPP1, the shaded cell strings are bypassed and only the unshaded ones generate power (red square marker in Figure 1(a)-(b)). On the other hand, at MPP2 all cell strings contribute to the power generation at the reduced current imposed by the shaded cell strings (green circle markers in Figure 1(a)-(b)).

Using the single-diode model, the equivalent circuit of the PV string is depicted in Figure 1(c) in black line color, comprising the unshaded (white background) and shaded (grey background) components. Each subcircuit employs a set of five parameters I_{ph}, I_s, a, R_s and R_{sh} for the single-diode model and the bypass diode *BP* coefficients I_{sbp}, a_{bp} (the subscript "un" or "sh" refers to the unshaded or shaded group respectively).

It is worth noting that, while operating at MPP1, the bypass diode of the unshaded cell strings BP_{un} is not conducting, while the p-n junction of the shaded cell strings D_{sh} is reverse biased. Therefore, the equivalent circuit for operation at MPP1 may be simplified as shown in Figure 1(d) in red color. Similarly, at MPP2, none of the bypass diodes conducts, leading to the simplified

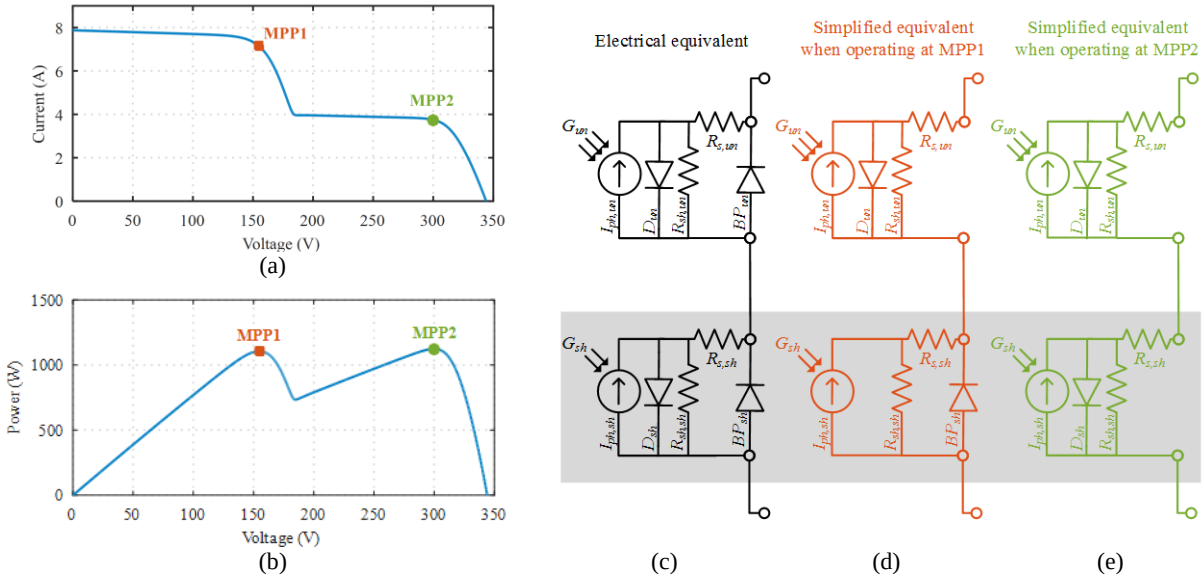

Figure 1. (a) *I-V* and (b) *P-V* characteristics of a PV string illuminated at two irradiance levels, (c) electrical equivalent circuit and (d)-(e) simplified equivalents for operation at MPP1 and MPP2 respectively.

equivalent depicted in Figure 1(e) in green color.

In order to describe the operation of the aforementioned circuits, the single-diode model equation is used [7], [9]:

$$V_{cs} = R_{sh} I_{ph} - \left(R_s + R_{sh}\right) I - aW\left\{\frac{R_{sh} I_s}{a} e^{R_{sh}\frac{I_{ph}-I}{a}}\right\} \quad (1)$$

where V_{cs} and the five parameters I_{ph}, I_s, a, R_s and R_{sh} refer to a *single* cell string. Eq. (1) is expressed in explicit form by means of the Lambert W function $W\{.\}$.

According to the above analysis, when operating at MPP1 the unshaded part of the string may be modeled through (1) (Figure 1(d)). On the other hand, the shaded component is bypassed, thus it is described by the bypass diode equation [7]:

$$V_{bp} = -a_{bp} \ln\left(\frac{I - I_{SC,sh}}{I_{sbp}}\right) \quad (2)$$

where $I_{SC.sh}$ is the short circuit current of the shaded cell strings, approximated as:

$$I_{SC,sh} = \frac{R_{sh,sh}}{R_{s,sh} + R_{sh,sh}} I_{ph,sh} \quad (3)$$

For MPP2 operation (Figure 1(e)), eq. (1) applies to both the shaded and unshaded part, albeit using different sets of five parameters. Therefore, the entire PV string equation is given by:

$$\begin{cases} \text{MPP1: } V_{str} = N_{un} V_{cs,\text{un}} - N_{sh} V_{bp} \\ \text{MPP2: } V_{str} = N_{un} V_{cs,un} + N_{sh} V_{cs,sh} \end{cases} \quad (4)$$

where V_{str} denotes the total string voltage, $V_{cs,un}/V_{cs,sh}$ is the voltage of one unshaded/shaded cell string using (1) and the respective five parameters, and V_{bp} is the voltage drop on the bypass diode via (2).

Eq. (4) describes the entire PV string when operating under two irradiance levels, depending on the actual operating region (MPP1 or MPP2). The parameters involved are: five parameters for the unshaded cell strings ($I_{ph,un}$, $I_{s,un}$, a_{un}, $R_{s,un}$ and $R_{sh,un}$), five parameters for the shaded ones ($I_{ph,sh}$, $I_{s,sh}$, a_{sh}, $R_{s,sh}$ and $R_{sh,sh}$), the coefficients of the two bypass diode (I_{sbp} and a_{bp}) and the number of shaded and unshaded cell strings (N_{sh} and N_{un}).

3 CURVE FITTING MPPT (CFMPPT) ALGORITHM

The main concept of the proposed algorithm is to estimate the aforementioned parameters by applying curve fitting on a set of past measurements. According to the previous analysis, the unknowns to be determined are 14 in total, which are too many to be determined via a curve fitting procedure. Given that the unshaded cell strings number is the complement of the shaded ones (N_{tot} = N_{sh}+N_{un}), and considering the bypass diodes' coefficients known and unaffected by the operating conditions, still there are 11 unknown parameters.

In order to further reduce the number of unknowns, the five parameters of each group are correlated with their STC values and the operating conditions (irradiance and temperature). For this, the extrapolation equations proposed in [10], as reworked in [11], are employed:

$$I_{ph0} = G\left(I_{ph0} + a_{Isc}\left(T - T_0\right)\right) \quad (5)$$

$$I_s = I_{s0}\left(\frac{T}{T_0}\right)^3 e^{47.1\left(1-\frac{T_0}{T}\right)} \quad (6)$$

$$a = a_0 \frac{T}{T_0} \quad (7)$$

$$R_s = R_{s0} \quad (8)$$

$$R_{sh} = \frac{R_{sh0}}{G} \quad (9)$$

where I_{ph0}, I_{s0}, a_0, R_{s0}, R_{sh0} denote the reference parameters (STC values), a_{Isc} is the temperature coefficient of the short circuit current (A/K) and T_0 = 298.15 K is the nominal temperature at STC. The incident irradiance is denoted as G (p.u.) and the cell temperature as T (K).

The five reference parameters at STC are known beforehand, calculated from datasheet information via a method such as the one proposed in [11]. Therefore, only the two irradiance levels and the temperature have to be determined in order to obtain all ten circuit parameters (a common cell temperature across the PV string is assumed). Consequently, the final *shading parameters* are limited to four: [G_{un}, G_{sh}, T, N_{sh}].

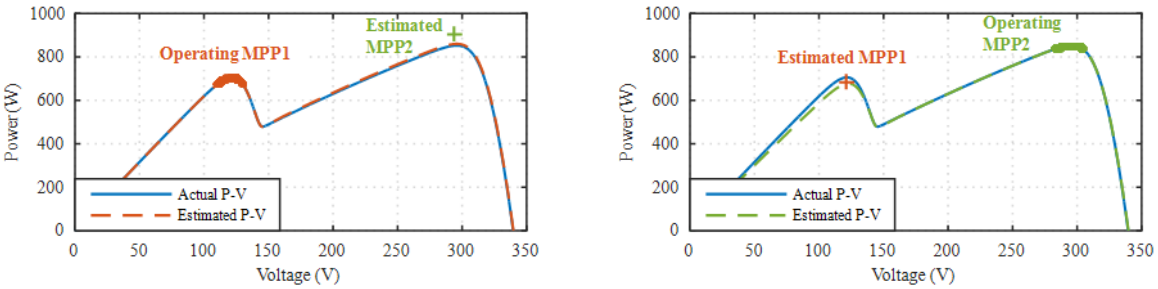

Figure 2. Operating point variation around (a) MPP1 and (b) MPP2, exploited in order to estimate the shading parameters and the other MPP.

These 4 parameters are determined by applying least squares curve fitting (LSQ CF) on a set of previous measurements [12], included in a *measurement window*. To facilitate understanding, an indicative scenario is illustrated in Figure 2(a). A standard P&O algorithm is constantly running, continuously perturbing the operating point of the PV string, thus creating a measurement window around MPP1 indicated by red circle markers in Figure 2(a). The LSQ CF method fits (4) (upper branch in this case) to the measurements in order to extract the shading parameters.

The resulting [G_{un}, G_{sh}, T, N_{sh}] are then used to calculate the other MPP's voltage and power (green cross marker in Figure 2(a))**,** using the simple expressions given in [7] and enhanced in [8] for arbitrary temperature:

$$\text{MPP1:}\begin{cases} V_{mp1} = N_{un} V_{mp}^{T} - N_{sh}\Delta V_{D} \\ I_{mp1} = G_{un} I_{mp}^{T} \end{cases} \tag{10}$$

$$\text{MPP2:}\begin{cases} V_{mp2} = N_{un}\left(\dfrac{G_{sh}}{G_{un}} V_{mp}^{T} + \left(1 - \dfrac{G_{sh}}{G_{un}}\right) V_{oc}^{T}\right) + N_{sh} V_{mp}^{T} \\ I_{mp2} = G_{sh} I_{mp}^{T}\left(1 + \lambda \dfrac{N_{un}}{N_{tot}}\right) \end{cases} \tag{11}$$

where V^{T}_{mp}, I^{T}_{mp} and V^{T}_{oc} are the MPP voltage, MPP current and open circuit voltage at *nominal irradiance but arbitrary temperature T*, ΔV_D denotes the voltage drop on one bypass diode (typically 1 V) and λ is an empirical coefficient equal to 0.06 [7]. The parameters V^{T}_{mp}, I^{T}_{mp} and V^{T}_{oc} are related to their nominal values via [8]:

$$\begin{aligned} I_{mp}^{T} &= I_{mp0} + \alpha_{Imp}\left(T - T_0\right) \\ V_{mp}^{T} &= V_{mp0} + \beta_{Vmp}\left(T - T_0\right) \\ V_{mp}^{T} &= V_{oc0} + \beta_{Voc}\left(T - T_0\right) \end{aligned} \tag{12}$$

where a_{Imp}, β_{Vmp} and β_{Voc} are the respective *absolute* temperature coefficients. If, a_{Imp} is not provided in the datasheet, it may be set equal to a_{Isc} or simply zero, while in the absence of β_{Vmp}, β_{Voc} may be used instead.

Using the shading parameters [G_{un}, G_{sh}, T, N_{sh}] and the aforementioned equations, the other MPP's voltage and current are determined. Thereafter, the operating point is shifted to MPP2, if the latter provides more power than the current operating point MPP1 (Figure 2(a)). A similar procedure is performed when operating at MPP2 (Figure 2(b)).

It is worth noting that the variation of the operating point around the current MPP is due to the inherent ripple caused by the switching of the DC/DC converter and the perturbation introduced by the P&O algorithm. The duration that corresponds to the samples of the measurement window is denoted window period T_{win}. It can be set from several tens to a few hundreds of milliseconds, to ensure curve fitting robustness and enhanced tracking capability of fast shade variations.

Regarding the calculation algorithm employed at LSQ CF, the Levenberg-Marquardt method is adopted which is an iterative procedure [13]. Nevertheless, in order to reduce computational cost and permit implementation in a simple microcontroller, *only one iteration* is executed in each step of the proposed CFMPPT algorithm, i.e. every T_{win}. A few iterations per second (one every T_{win}) are sufficient to continuously adapt to the varying environmental conditions, even the most rapidly changing ones.

The flowchart of the proposed CFMPPT technique is illustrated in Figure 3. It is worth noting that a standard P&O is constantly in operation, in order to continuously fine tune the operating point and create the measurement window required by the CFMPPT algorithm. The latter is executed at a lower frequency, to track the MPPs and ensure operation at the global maximum at all times.

At each cycle of the CFMPPT execution (Figure 3), the ten circuit parameters (five for the shaded and five for the unshaded group) are first extrapolated to the previously estimated irradiance and temperature values, applying the equations (5)-(9). Thereafter, a *single iteration* of the LSQ CF algorithm is performed (Levenberg-Marquardt) to update the shading parameters using the upper or lower branch of (4), depending on the current MPP.

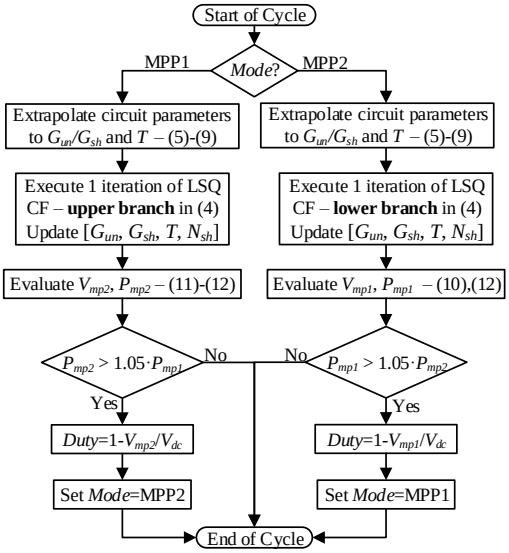

Figure 3. Flowchart of proposed CFMPPT technique: it detects the actual shading parameters and properties of all MPPs and manages transitions to global MPP.

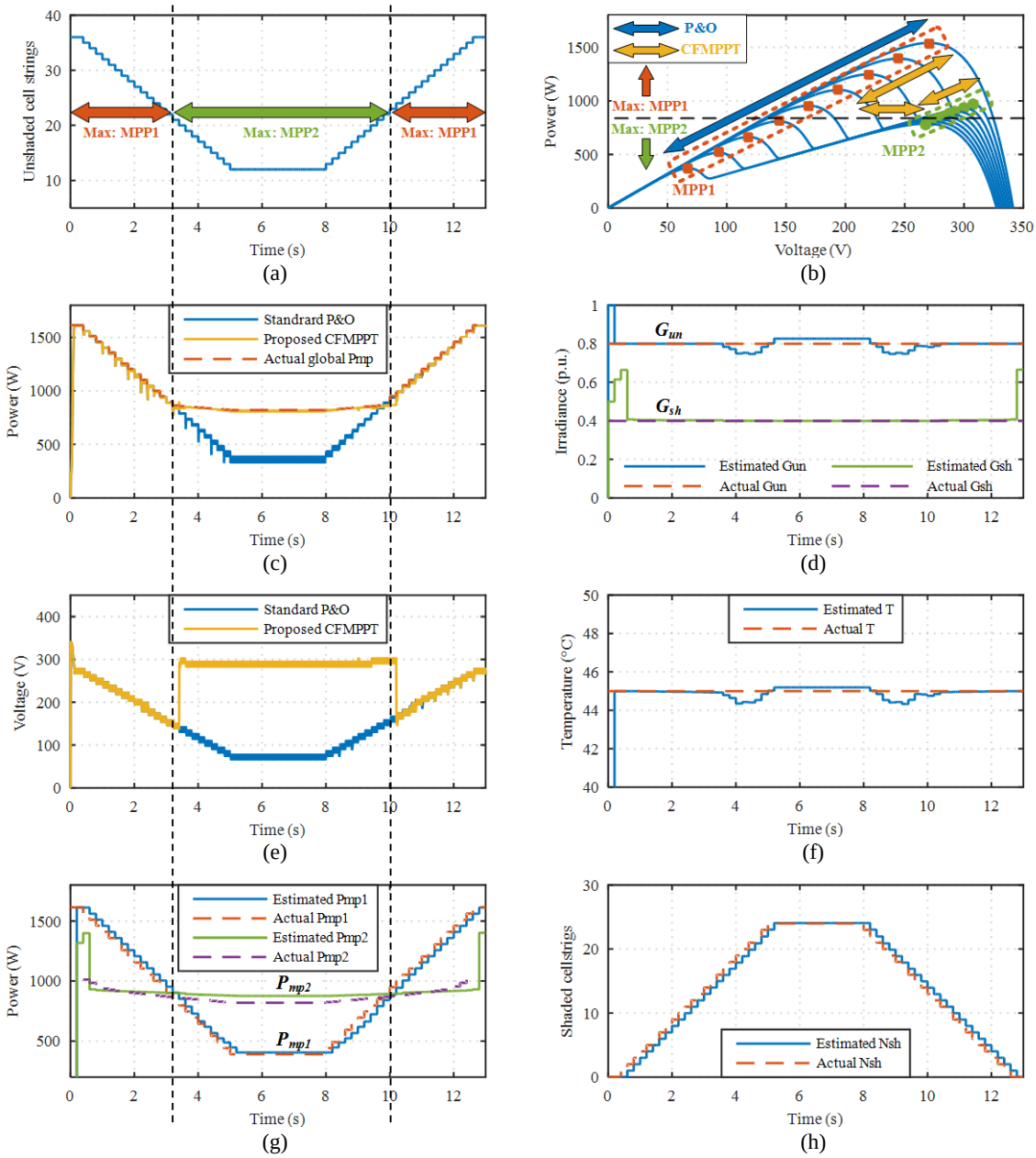

Figure 4. Simulations of a partially shaded PV string with G_{un}=0.8, G_{sh}=0.4 and T=45°C at varying N_{sh}=0-24 of 36 cell strings in total, applying a standard P&O algorithm and the proposed CFMPPT method. (a) Unshaded cell strings N_{un}, (b) *P-V* curve variation, (c) output power, (d) estimated irradiance values G_{un} and G_{sh}, (e) operating voltage, (f) estimated temperature T, (g) estimated P_{mp1} and P_{mp2}, and (h) estimated shaded cell strings number N_{sh}.

Subsequently, the other MPP's voltage and power are evaluated through (10)-(12) and compared to the actual operating point in terms of power levels: if the deviation is more than a tolerance limit (e.g. 5%), then a transition to the other MPP is performed. In Figure 3, the duty cycle is calculated for a boost converter, utilizing the target voltage and the voltage level of the DC link V_{dc}.

4 SIMULATIONS

In order to study the proposed CFMPPT algorithm and compare its effectiveness to a standard P&O method, simulations are performed in MATLAB/Simulink. A PV string composed by 12 PV modules is considered, each having 3 bypass diodes (36 cell strings in total), partially shaded at varying extent up to 66% of the total area (N_{un}=12-36 in Figure 4(a)). The window period T_{win} is set to 100 ms, while the internal P&O operation is executed every 10 ms. The irradiance on the unshaded and shaded groups is G_{un} = 0.8 and G_{sh} = 0.4 respectively (50% shadow intensity), while the common temperature T = 45 °C. A rapidly changing shading event has been considered with a duration of only 13 seconds. As shown in Figure 4(a), MPP1 is the global maximum at the time intervals 0-3.2 s and 10-13 s (red arrows), whereas MPP2 provides more power at the rest of the duration (green arrow).

The *P-V* curve variation over time is illustrated in Figure 4(b) in blue colored curves, indicating MPP1 and MPP2 with red square and green circle markers respectively. While the system is unshaded, the standard P&O method operates at the sole MPP of the *P-V* curve

(upper red square marker MPP1). As the shadow appears and extends, the P&O continuously fine tunes the operating point around MPP1 while it shifts to lower voltages. Essentially, the algorithm is locked at this MPP for the entire duration of the event (blue arrow in Figure 4(b)), even when it is not the global one. On the contrary, the developed CFMPPT initially operates at MPP1, but always keeps track of MPP2, switching to the latter when MPP1 is no longer the global maximum, as the orange arrows indicate in Figure 4(b).

This is clearly illustrated in Figure 4(c), where the output power over time is depicted. While the typical P&O (blue color) stays locked on MPP1 for the entire duration, the CFMPPT method (orange color) performs a transition to MPP2 at t = 3.4 s and back to MPP1 at t = 10.2 s, guaranteeing optimal operation throughout the simulation. This way, it provides output power almost identical to the maximum possible (red dashed line). Consequently, the MPPT efficiency of the standard P&O algorithm is measured 83.5% for this particular scenario, as opposed to 98.2% of the proposed CFMPPT method (the small deviation from 100% is due to the unavoidable ripple of the operating point). Notably, the CFMPPT algorithm performs reliably even for fast illumination transients, lasting only a few seconds, as would occur during fast moving cloud conditions.

The operating voltage when applying the two methods is depicted in Figure 4(e). The standard P&O algorithm (blue line) follows the variation of MPP1 voltage, which is proportional to the unshaded area (Figure 4(a)). On the other hand, the operating voltage at the CFMPPT technique presents two distinct levels that correspond to the two different MPPs. The short delay in the transitions is associated to the duration of the window period T_{win}.

Regarding the accuracy in the calculation of the shading parameters, the estimated and actual irradiance levels G_{un} and G_{sh} are depicted in Figure 4(d). After t = 0.2 s, the estimated G_{un} (continuous blue line) coincides with its actual value (red dashed line) as long as the operating point is MPP1, while a small deviation is observed during operation at MPP2. In the latter case, the effect of the unshaded group is quite limited and thus the parameters of this group (G_{un}) are more difficult to be extracted by curve fitting. Similarly, the G_{sh} estimation in the same figure (green continuous line) is perfectly aligned with the actual irradiance (purple dashed line), as long as at least one cell string is shaded. When there is no shadow at all (0-0.6 s and 12.8-13 s), G_{sh} takes arbitrary/meaningless values, yet always lower than G_{un}.

In Figure 4(f), the estimated temperature T (blue continuous line) quickly converges to its actual value (red dashed line) within the first 0.2 s. During the rest of the simulation, a slight deviation is observed from 3.4 to 10.2 s, for the same reasons as G_{un}. Regarding the number of shaded cell strings N_{sh} in Figure 4(h), perfect coincidence between actual and estimated values is observed, albeit with a small time delay associated with the window period T_{win}.

As a result, the estimation of the two MPPs power is quite satisfactory in Figure 4(g). The estimated P_{mp1} (blue line) presents a small delay compared to its actual value (red dashed line), due to N_{sh} calculation (Figure 4(h)). Similarly, P_{mp2} (green line) takes meaningless values when the system is unshaded. Overall, the proposed CFMPPT algorithm correctly determines the global maximum power over the entire duration, performing the appropriate transitions of the operating point when needed.

5 CONCLUSIONS

In this paper, a new MPPT strategy for a PV string under partial shading is introduced, which applies curve fitting on electrical measurements recorded by the dc/dc converter, to continuously monitor the global maximum. The method is capable of tracking fast shading variations, while it introduces minimum additional perturbation to the operation of the PV string. The proposed algorithm supports any temperature and irradiance (two different irradiance levels) and is readily implementable in a microprocessor. The simulations presented validate its superiority over a standard P&O approach.

6 ACKNOWLEDGMENTS

Mr. E. Batzelis and Mr. G. Kampitsis are supported in their PhD studies by "*IKY Fellowships of Excellence for Postgraduate Studies in Greece - Siemens Program*".

7 REFERENCES

[1] H. Patel and V. Agarwal, "Maximum power point tracking scheme for PV systems operating under partially shaded conditions," *IEEE Trans. Ind. Electron.*, vol. 55, no. 4, pp. 1689–1698, Apr. 2008.

[2] Y.-H. Ji, D.-Y. Jung, J.-G. Kim, J.-H. Kim, T.-W. Lee, and C.-Y. Won, "A real maximum power point tracking method for mismatching compensation in PV Array under partially shaded conditions," *IEEE Trans. Power Electron.*, vol. 26, no. 4, pp. 1001–1009, Apr. 2011.

[3] K. Ishaque, Z. Salam, M. Amjad, and S. Mekhilef, "An improved particle swarm optimization (PSO)–based MPPT for PV with reduced steady-state oscillation," *IEEE Trans. Power Electron.*, vol. 27, no. 8, pp. 3627–3638, Aug. 2012.

[4] E. Koutroulis and F. Blaabjerg, "A new technique for tracking the global maximum power point of PV arrays operating under partial-shading conditions," *IEEE J. Photovoltaics*, vol. 2, no. 2, pp. 184–190, Apr. 2012.

[5] M. Miyatake, M. Veerachary, F. Toriumi, N. Fujii, and H. Ko, "Maximum power point tracking of multiple photovoltaic arrays: A PSO approach," *IEEE Trans. Aerosp. Electron. Syst.*, vol. 47, no. 1, pp. 367–380, Jan. 2011.

[6] E. Batzelis and S. Papathanassiou, "An efficient MPPT algorithm for partially shaded PV strings," in *Proc. 31st Eur. Photovolt. Sol. Energy Conf. Exhib. (EU PVSEC 2015)*, Hamburg, Germany, Sep. 2015, pp. 1615–1619.

[7] E. I. Batzelis, I. A. Routsolias, and S. A. Papathanassiou, "An explicit PV string model based on the Lambert W function and simplified MPP expressions for operation under partial shading," *IEEE Trans. Sustain. Energy*, vol. 5, no. 1, pp. 301–312, Jan. 2014.

[8] G. N. Psarros, E. I. Batzelis, and S. A. Papathanassiou, "Partial shading analysis of multistring PV arrays and derivation of simplified MPP expressions," *IEEE Trans. Sustain. Energy*, vol. 6, no. 2, pp. 499–508, Apr. 2015.

[9] E. I. Batzelis, G. E. Kampitsis, S. A. Papathanassiou, and S. N. Manias, "Direct MPP calculation in terms

of the single-diode PV model parameters," *IEEE Trans. Energy Convers.*, vol. 30, no. 1, pp. 226–236, Mar. 2015.

[10] W. De Soto, S. A. Klein, and W. A. Beckman, "Improvement and validation of a model for photovoltaic array performance," *Sol. Energy*, vol. 80, no. 1, pp. 78–88, Jan. 2006.

[11] E. I. Batzelis and S. A. Papathanassiou, "A method for the analytical extraction of the single-diode PV model parameters," *IEEE Trans. Sustain. Energy*, vol. 7, no. 2, pp. 504–512, Apr. 2016.

[12] "Least squares." [Online]. Available: http://en.wikipedia.org/wiki/Least_squares.

[13] "Levenberg-Marquardt algorithm." [Online]. Available: https://en.wikipedia.org/wiki/Levenberg-Marquardt_algorithm.